International Journal of Nanomedicine

Dovepress
open access to scientific and medical research

Open Access Full Text Article

ORIGINAL RESEARCH

Biocompatibility and antibacterial activity of nitrogen-doped titanium dioxide nanoparticles for use in dental resin formulations

This article was published in the following Dove Press journal:
International Journal of Nanomedicine
5 December 2016
Number of times this article has been viewed

Andrew Zane[1]
Ranfang Zuo[2]
Frederick A Villamena[3]
Antal Rockenbauer[4,5]
Ann Marie Digeorge Foushee[1]
Kristin Flores[1]
Prabir K Dutta[2]
Amber Nagy[1]

[1]Biomaterials and Environmental Surveillance Department, Naval Medical Research Unit San Antonio, Joint Base San Antonio, Fort Sam Houston, San Antonio, TX, [2]Department of Chemistry and Biochemistry, [3]Department of Biological Chemistry and Pharmacology, Davis Heart and Lung Research Institute, College of Medicine, The Ohio State University, Columbus, OH, USA; [4]Research Centre for Natural Sciences of the Hungarian Academy of Sciences, Institute of Materials and Environmental Chemistry, [5]Department of Physics, MTA-BME Condensed Matter Research Group, Budapest University of Technology and Economics, Budapest, Hungary

Abstract: The addition of antibacterial functionality to dental resins presents an opportunity to extend their useful lifetime by reducing secondary caries caused by bacterial recolonization. In this study, the potential efficacy of nitrogen-doped titanium dioxide nanoparticles for this purpose was determined. Nitrogen doping was carried out to extend the ultraviolet absorbance into longer wavelength blue light for increased biocompatibility. Titanium dioxide nanoparticles (approximately 20–30 nm) were synthesized with and without nitrogen doping using a sol–gel method. Ultraviolet–Visible spectroscopy indicated a band of trap states, with increasing blue light absorbance as the concentration of the nitrogen dopant increased. Electron paramagnetic resonance measurements indicated the formation of superoxide and hydroxyl radicals upon particle exposure to visible light and oxygen. The particles were significantly toxic to *Escherichia coli* in a dose-dependent manner after a 1-hour exposure to a blue light source (480 nm). Intracellular reactive oxygen species assay demonstrated that the particles caused a stress response in human gingival epithelial cells when exposed to 1 hour of blue light, though this did not result in detectable release of cytokines. No decrease in cell viability was observed by water-soluble tetrazolium dye assay. The results show that nitrogen-doped titanium dioxide nanoparticles have antibacterial activity when exposed to blue light, and are biocompatible at these concentrations.

Keywords: titanium dioxide, antibacterial activity, nitrogen doping

Introduction

Despite the long-term environmental and human health concerns related primarily to mercury, amalgam dental restorations are still widely used. This is due to their enhanced durability over composite resins, particularly in the case of large restorations placed in molars.[1] Failure of composite resin restorations is typically the result of two major factors: errors during placement, such as inadequate or uneven curing, and secondary caries caused by shrinkage and breakage of the material leading to colonization of biofilm-forming bacteria in the resin–dentin interface.[2] A 2003 review[3] found that these failures are due to improper placement technique or incorrect choice of materials when they occur within the first 5 years after placement. Failures occurring between 5 and 17 years are typically the result of secondary caries. Overall failure rates during this time period are as high as 45%.[3]

The acidic conditions associated with secondary caries primarily affect the remaining tooth, but not the restoration material.[4] *Streptococcus mutans* biofilms grown on a resin–dentin interface cause a significant reduction in fatigue resistance of the joint material due to degradation of dentin at the resin–dentin interface.[5] The incorporation

Correspondence: Amber Nagy
Naval Medical Research Unit San Antonio, 3650 Chambers Pass, JBSA Ft. Sam Houston, San Antonio, TX 78234, USA
Tel +1 210 539 7017
Email amber.m.mallory2.civ@mail.mil

submit your manuscript | www.dovepress.com
Dovepress
http://dx.doi.org/10.2147/IJN.S117584

of an antibacterial agent into this region, which is inaccessible during typical oral prophylaxis, will reduce dental restoration failure and increase their effective lifetime. Traditional organic molecules used as antibacterial agents are not ideal for this application, as they have limited stability and lifetimes. Inorganic materials with antibacterial activity have generally longer usable lifetimes, and thus have greater potential for successful use in this case.

The development of nanomaterials, materials smaller than 100 nm in at least one dimension, has resulted in advancements in many fields, including the improvement of antibacterial and "self-cleaning" properties of materials such as concrete,[6] glass,[7] and medical devices and materials.[8–10] TiO_2 has been extensively used in the development of these materials due to photocatalytic activity stimulated by ultraviolet (UV) light exposure. Upon excitation with UV light, TiO_2 generates reactive oxygen species (ROS) in the presence of water.[11] The ROS generated in this reaction lead to the decomposition of organic compounds[11] and have demonstrated antibacterial activity toward several bacterial strains including *Escherichia coli*, *Pseudomonas aeruginosa*, and *Staphylococcus aureus*.[12–14]

Nanoparticles, primarily silica and zirconium oxide, are currently used in dental composite resins to increase the strength properties while reducing material shrinkage during curing.[15] There is a clear opportunity to replace these with functionalized nanomaterials that could impart additional benefits, such as antibacterial TiO_2. Recently, an antibacterial composite was developed that also had self-healing and remineralization properties using calcium phosphate nanoparticles.[16] Another self-healing composite material was developed using breakable capsules of unreacted monomers, which has shown promising healing characteristics.[17]

Recent research has shown that the light absorption of TiO_2 can be shifted to the visible range by doping with a variety of atoms, including nitrogen,[18–21] fluorine,[22] copper,[23] and silver,[24] resulting in a new class of visible light active materials. This is of particular interest in the development of novel dental materials for two reasons: exposure of gum tissue to blue light is preferable to cytotoxic UV light[25] and most of the dental offices are already equipped with blue light sources used to cure photoactive composite dental resins. The incorporation of blue light–sensitive TiO_2 into a dental material could allow for long-term and repeatable release of antibacterial ROS. This is currently not possible with traditional commercially available organic antibiotics, which are consumed upon use.

Techniques for doping of TiO_2 to increase the UV and visible light sensitivity initially utilized metals. This was generally unsuccessful due to issues with reproducibility and lack of photocatalytic activity at visible wavelengths, attributed to high carrier recombination rates.[26] Later, nonmetal-doped TiO_2 was developed, primarily with nitrogen, which is to date the most successful and widely utilized dopant for the visible light sensitization of titania.[27] Nitrogen-doped TiO_2 with codopants such as silver has also been developed with promising characteristics.[24] Metal dopants or codopants are, however, not ideal for eventual clinical use due to the potential for metal leaching and toxicity to the surrounding tissue when used at concentrations necessary for killing pathogenic bacteria.[28,29]

In this report, nitrogen-doped TiO_2 particles (N-TiO_2 NPs) were synthesized based on a representative literature source[18] for potential incorporation into a novel dental resin material with light-activated antibacterial properties. N-TiO_2 NPs were extensively characterized by various techniques. To determine if the particles are appropriate for further study toward this application, their toxicity under blue light (485 nm) exposure to a model bacterium, *E. coli*, and their biocompatibility with human gingival epithelial cells (hGEPs) were examined.

Methods

Chemical synthesis and characterization

N-TiO_2 synthesis

Synthesis of N-TiO_2 NPs was adapted from a recent literature synthesis,[18] wherein a sol–gel synthesis of TiO_2 was modified to add ethylmethylamine as a nitrogen source.

Titanium isopropoxide, anhydrous ethanol, hydrogen peroxide (30%, w/v), and ethylmethylamine were all purchased from Sigma Aldrich and used without further purification. The water used in the procedure was purified by a Millipore Milli-Q Advantage A-10 Water Purification System.

Titanium tetraisopropoxide (5 g) was first added to 10 mL anhydrous ethanol in a dry inert (nitrogen) environment. This mixture was added to 50 mL of water while stirring (600 rpm), which forms a white TiO_2 precipitate instantaneously. Stirring was continued for an additional 10 minutes after which point the precipitate was washed with water three times by centrifugation (5,000× *g*).

In a fume hood, 10 mL of 30% (w/v) hydrogen peroxide was added to the washed precipitate while stirring (600 rpm), which results in the formation of an orange transparent solution after several minutes. After dissolution, 0.104 g ethylmethylamine was added and the solution was then stirred

overnight until it thickened into a gel. The gel was dried for 24 hours at 100°C, and then ground into a powder using a mortar and pestle. The resulting powder was then calcined at 300°C in a muffle furnace for 24 hours. To determine the impact of nitrogen precursor concentration on doping levels, the amount of ethylmethylamine added was varied as 0, 0.104, 0.130, and 0.156 g. The final samples were labeled 1, 1.25, and 1.5 N-TiO_2, respectively, signifying the relative amount of nitrogen added based on the literature synthesis.[18]

Importantly, care should be taken, particularly at higher concentrations of ethylmethylamine or if attempting to scale up this synthesis, as ethylmethylamine is unstable and ignitable. While the 1.5 N-TiO_2 NP sample was found to absorb the most visible light, a subsequent batch of these particles ignited during the calcination step, presumably due to an excess of unreacted ethylmethylamine. Also, 1.25 N-TiO_2 NPs were synthesized without any untoward incident, and the majority of experiments detailed below were carried out with this nitrogen loading ratio. When scaling up the synthesis, this issue could potentially occur at lower ethylmethylamine concentrations without proper ventilation.

Particle characterization

Diffuse reflectance UV–Visible (UV–Vis) absorption spectra of all samples were recorded from 400 to 800 nm using a Shimadzu UV-2501PC spectrophotometer with ISR-2200 diffuse reflectance attachment.

Zeta potential measurements were recorded with a Malvern Zetasizer Nano ZS. The pH titrations were performed with an attached MPT-2 titrator supplied with 1 M hydrochloric acid. Titration samples were preadjusted to a pH between 11 and 12 by adding 1 M sodium hydroxide dropwise, sonicated, and allowed to rest for 30 minutes. Three zeta potential measurements were taken at approximately 0.2 pH unit intervals between pH 11 and 4, with 30 seconds resting time between each measurement. Zeta potential measurements include a minimum of 10 runs in monomodal mode and were analyzed using Smoluchowski model.

High-resolution transmission electron microscopy (TEM) images were obtained using a Tecnai-F20 system. Particles were washed twice by centrifugation and replacement of supernatant with deionized water. The particles were then suspended in a dilute ethanol solution and deposited onto lacey carbon–coated copper grids. Primary particle sizes were evaluated using ImageJ software, measuring at least 50 particles for each sample.

Electron paramagnetic resonance (EPR) spectroscopic measurements were carried out on a Bruker X-band spectrometer with a high-sensitivity resonator at room temperature. General instrument settings were as follows: microwave power, 10 mW; modulation amplitude, 1 G; receiver gain 1×10^5; time constant, 82 milliseconds; and time sweep, 42 seconds. Using the spin trap, 5,5-dimethyl-1-pyrroline-*N*-oxide (DMPO), radical adducts were identified from dispersed particles in both aqueous and dimethyl sulfoxide (DMSO) solutions.[30] In a typical experiment, approximately 13–14 mg of doped 1.25 N-TiO_2 in 100 µL distilled water or DMSO suspension was prepared. Equal volumes (25 µL) of TiO_2 suspension (aqueous or in DMSO) and DMPO solution were thoroughly mixed to give a final DMPO concentration of 100 mM. For DMSO experiments, the suspension was bubbled with air, oxygen, or argon for 5 minutes. The resulting suspensions were transferred to 50 µL capillary tubes and placed inside the sample cavity. The suspensions were irradiated inside the sample cavity using a fiber-optic 150 W quartz halogen visible light source. The hyperfine splitting constants of the spin adducts were determined by simulating the spectra using an automatic fitting program.[31]

Powder X-ray diffraction patterns of doped and undoped TiO_2 NPs were collected on a Rigaku Geigerflex diffractometer using Ni-filtered Cu Kα radiation at 40 kV and 25 mA at 2θ from 20° to 70°.

Biological studies

Cell culture and N-TiO_2 NP exposures

Pooled primary hGEPs were purchased from CellnTec Advanced Cell Systems AG (Stauffacherstr, Switzerland) and propagated in CnT-Prime epithelial culture medium (CellnTec Advanced Cell Systems AG) on 100 mm petri dishes coated with 30 µg/mL Type I rat tail collagen (BD Biosciences, Bedford, MA, USA) diluted in Dulbecco's phosphate-buffered saline. This cell type was chosen since N-TiO_2 NPs have the potential to serve as a component in dental resin formulations, thereby putting them in close contact with hGEPs. Cells were passaged when they reached 70%–90% confluency. For routine cultivation, the medium was changed approximately every 3 days. For viability and ROS production assays, cells from passages 3–7 were seeded at 2.5×10^4 cells per well in 96-well flat-bottomed tissue culture plates and acclimated overnight at 37°C, 5% CO_2 before N-TiO_2 NP exposure. N-TiO_2 NPs at 50, 100, and 200 µg/mL concentration were prepared in CnT-Prime media along with appropriate controls and added immediately to aspirated wells. Cells and nanoparticles were exposed to 485 nm at a constant power of 12.85 mW/cm^2 and a distance of 55 mm or ambient light for 60 minutes.

Temperatures for both light exposure conditions ranged between 30°C and 34°C. Biological experiments were performed with N-TiO_2 only as TiO_2 NPs did not show absorption in the blue light range.

Cell viability assays

Mitochondrial activity in hGEPs, as measured using water-soluble tetrazolium dye (WST-1) (Roche, Indianapolis, IN, USA), was assessed after incubation with no NPs (negative control), N-TiO_2 NPs, or 1% Triton X (positive control) following 60-minute light exposure. After removal of N-TiO_2 NPs by aspiration and culture media replenishment, WST-1 reagent was added to each well (10 µL) of 96-well plates. The plates were briefly tapped to ensure homogeneous reagent mixture and then incubated at 37°C and 5% CO_2 for 2 hours before reading at an absorbance wavelength of 440 nm and a reference wavelength of 600 nm.

Oxidative stress

ROS formation in hGEPs exposed to increasing concentrations of N-TiO_2 NPs was quantified using 5-(and-6)-carboxy-2′,7′-dichlorodihydrofluorescein diacetate, acetyl ester (CM-H_2DCFDA) (Molecular Probes, Eugene, OR, USA). hGEPs exposed to Dulbecco's phosphate-buffered saline only or H_2O_2 served as controls. N-TiO_2 NPs at all concentrations were included in wells without cells to determine potential induction of spontaneous fluorescence of CM-H_2DCFDA. Fluorescence was measured immediately after light exposures using an excitation wavelength of 490 nm and an emission wavelength of 535 nm at 0, 30, and 60 minutes postexposure.

N-TiO_2 NP antibacterial activity against *E. coli*

The goal of this research was to test the antibacterial activity of N-TiO_2 NPs in suspension before moving onto more complex biofilm models. Although *E. coli* is rarely associated with caries formation, other Gram-negative bacteria such as *Porphyromonas gingivalis* are frequently found in the oral cavity and can cause certain oral diseases, including gingivitis. Therefore, *E. coli* was chosen as a model bacterium to represent Gram-negative bacteria. Bacterial suspensions of *E. coli* were grown overnight in lysogeny broth (LB) media and diluted to an approximate concentration of 1×10^5 colony forming units/mL in phosphate-buffered saline (PBS). The suspended bacteria were plated in triplicate with the concentrations of particles ranging from 0 to 200 µg/mL. The bacteria were then exposed to ambient room light for 60 minutes as a control or to 485 nm at a constant power of 12.85 mW/cm^2 and a distance of 55 mm inside a custom-made light box. After light exposures, the bacteria were recovered for 5 hours at 37°C, serially diluted in PBS, and plated on LB agar plates for colony count measurements.

For confocal microscopy experiments, *E. coli* were suspended at a concentration of 1×10^5 colony forming units/mL in 24-well plates in LB media. Bacteria were then pelleted, aspirated, and resuspended with N-TiO_2 NPs suspended in LB media at a concentration of 50, 100, and 200 µg/mL. The plates were exposed to ambient or blue light (as described above) for 60 minutes. Bacteria were then stained with LIVE/DEAD® BacLight stain (Life Technologies, Philadelphia, PA, USA) by incubating them with 1:1 ratios of propidium iodide and SYTO 9 in LB media for 30 minutes in the dark before imaging with a Nikon Eclipse TE-2000E confocal microscope. In the confocal images, green staining is indicative of viable bacteria, whereas red staining represents dead bacteria.

Statistical analyses

All hGEP and *E. coli* experiments were repeated three independent times, with a minimum of three technical replicates per experiment.

Statistical comparisons were performed using GraphPad Prism 6 (GraphPad Software, Inc., La Jolla, CA, USA). Two-way analysis of variance with Tukey's multiple comparisons tests were used to determine if significant changes existed between light treatments as well as NP doses. Data were represented as mean ± standard deviation. Data were considered statistically significant if $P<0.05$.

Results

Particle characterization

To determine the effects of nitrogen doping on the absorption spectrum of TiO_2, UV–Vis diffuse reflectance experiments were performed. Figure 1A shows the UV–Vis diffuse reflectance spectra of TiO_2 with various amounts of nitrogen doping. Visible light absorption (from 400 to 800 nm) was enhanced with increasing nitrogen doping. Figure 1B shows Tauc plots of the UV–Vis absorption data, which are used to determine the bandgap of each sample. The bandgap was 3.11 eV for undoped, 1 N-TiO_2, and 1.25 N-TiO_2. This shifted to 2.99 eV for 1.5 N-TiO_2. Because of the adequate visible absorption by 1.25 N-TiO_2, and the problems with ignition of the 1.5 N-TiO_2 sample, all further experiments were carried out with 1.25 N-TiO_2.

To determine whether the addition of nitrogen affected the final crystal structure of the particles, X-ray diffraction

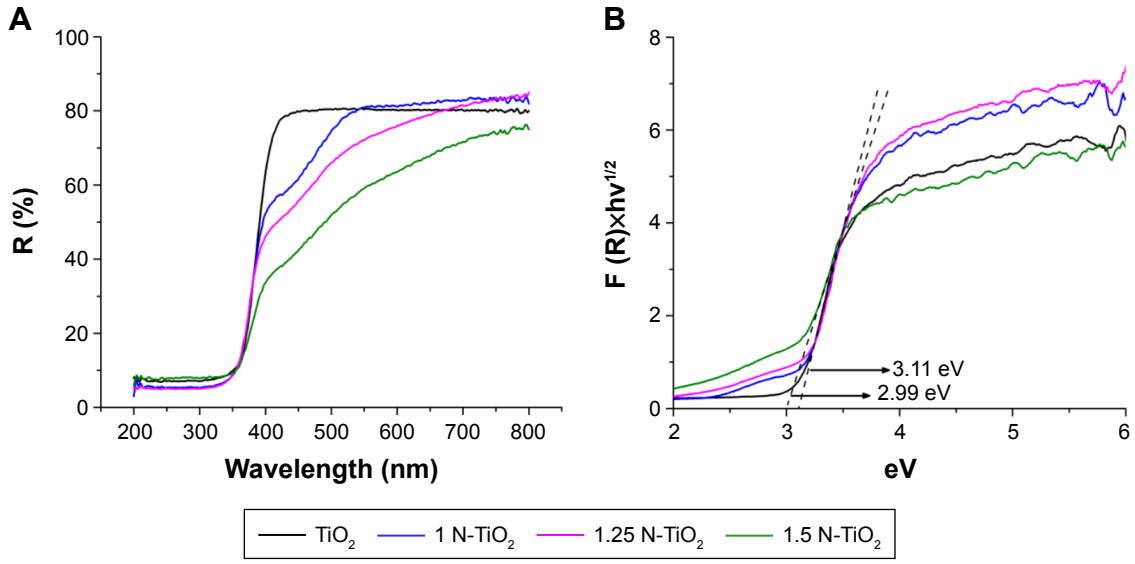

Figure 1 UV–Visible light absorption spectra of TiO_2 with increasing nitrogen content.
Note: (**A**) UV–Vis reflectance spectra and (**B**) Tauc plots of pure TiO_2 and N-TiO_2.
Abbreviations: UV, ultraviolet; Vis, visible.

patterns of undoped TiO_2 and N-TiO_2 were measured. These are shown in Figure 2 with anatase and rutile TiO_2 peaks labeled as "a" and "r", respectively. It is clear from the peak assignments that nitrogen doping resulted in the formation of primarily rutile phase TiO_2, while undoped TiO_2 was primarily anatase.

Particle size was determined by TEM. The TEM images shown in Figure 3 indicate irregular particle sizes and strong aggregation, which did not break apart after extensive sonication. Both the undoped (Figure 3A and B) and 1.25 N-TiO_2 NP samples (Figure 3C) consisted of aggregates ranging from 100 to 300 nm, made up of smaller primary particles: 33.1±10.3 nm for undoped TiO_2 and 21.8±9.6 nm for 1.25 N-TiO_2.

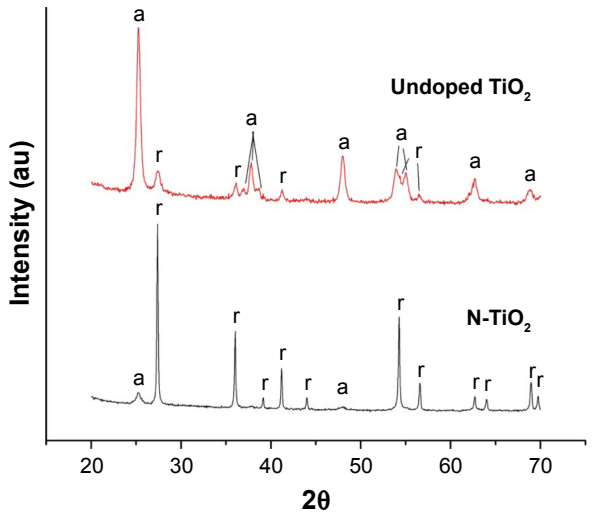

Figure 2 X-ray diffraction patterns of undoped and doped 1.25 N-TiO_2.
Note: Anatase phase titania peaks are marked "a", rutile phase titania peaks are marked "r".

The influence of nitrogen doping on the surface property of TiO_2 was explored with zeta potential versus pH titrations. The isoelectric point (IEP), or the pH at which the particles have a zero zeta potential, was determined to be at pH 5.2 for undoped TiO_2 NPs, while the N-TiO_2 NPs had the IEP shifted to a lower pH of 4.

EPR spectra were measured to specifically identify the radical species generated from particles upon exposure to visible light (approximately 400–675 nm). Figure 4 shows the hydroxyl adducts formed from 1.25 N-TiO_2 in the presence of DMPO under light irradiation. The concentration of N-TiO_2 was 136 mg/mL. No EPR signal was observed without irradiation (Figure 4A), while the signal formation was evident postirradiation (Figure 4B), which matched the simulation data for hydroxyl radical (Figure 4C).

Superoxide adduct has been shown to persist longer in DMSO than in aqueous solution.[33] Therefore, an experiment was carried out in DMSO to investigate $O_2^{\bullet-}$ generation. Also, in order to determine the potential role of dissolved O_2 in $O_2^{\bullet-}$ generation, the experiments were performed with air, Ar, or O_2 bubbling throughout the suspension.

Figure 5 shows the EPR using N-TiO_2 NPs in the presence of DMSO. No EPR signal was observed before irradiation, as shown in Figure 5A. The spectra for both air- and O_2-bubbled suspensions in the presence of irradiation (Figure 5B) are characterized by the presence of carbon-centered radical as

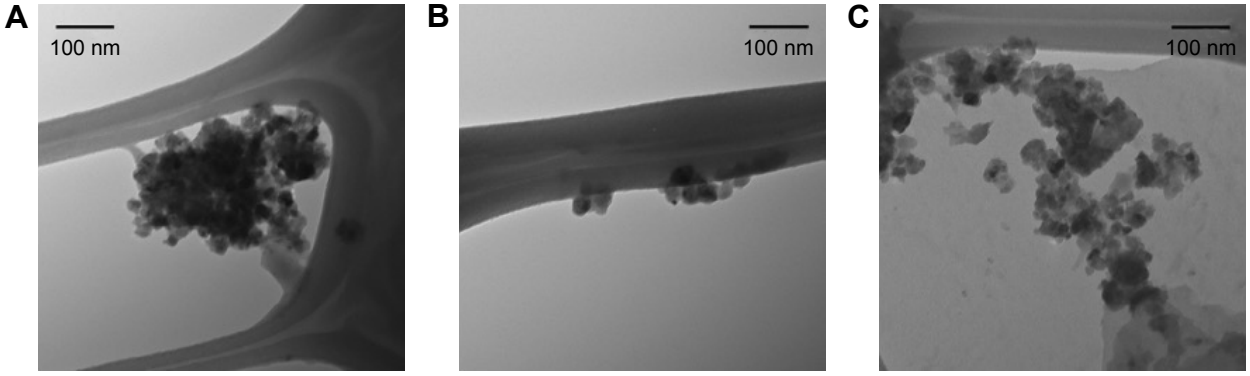

Figure 3 TEM images of (**A**, **B**) undoped TiO_2 and (**C**) 1.25 N-TiO_2.
Abbreviation: TEM, transmission electron microscopy.

$^{\bullet}CH_3$ and $O_2^{\bullet-}$ (as $^{\bullet}OOH$ adducts), as shown in the simulated spectra in Figure 5C.

Biocompatibility and antibacterial studies

To investigate the biocompatibility of N-TiO_2 NPs with hGEPs, the oxidative stress response of hGEPs after exposure to N-TiO_2 NPs under ambient light or 485 nm blue light was determined by a fluorescence ROS assay. Figure 6 illustrates the ROS production of hGEPs after exposure to N-TiO_2 NPs under ambient light (Figure 6A) and 485 nm blue light (Figure 6B). The cells produced ROS in response to blue light in the absence of N-TiO_2 NPs. This was accounted for by normalizing NP-exposed cells to the unexposed controls for both time points and light treatments. ROS generation significantly increased in a dose-dependent manner in the presence of blue light treatment.

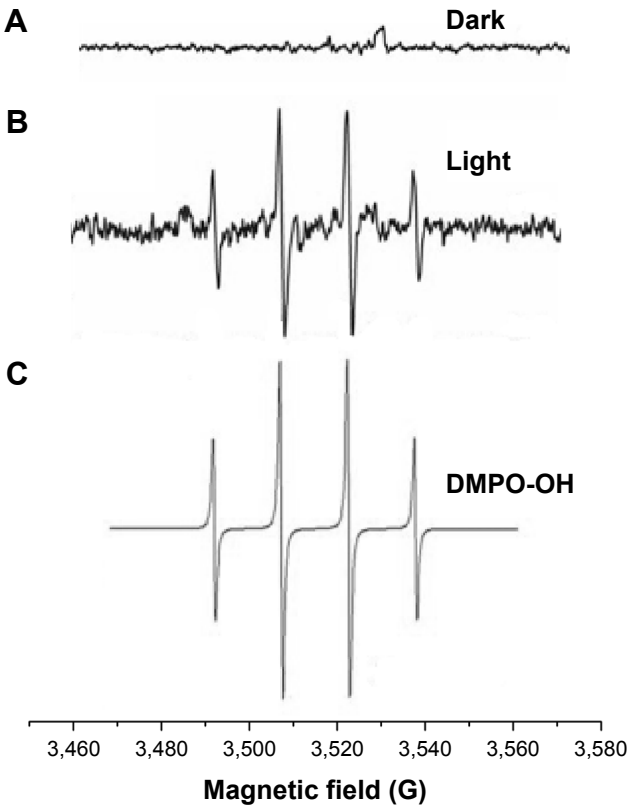

Figure 4 DMPO spin-trapping EPR spectra of 1.25 N-TiO_2 aqueous solutions under (**A**) dark conditions, (**B**) visible light irradiation, and (**C**) DMPO simulation (DMPO-OH: $a_N=a_{\beta-H}=14.9$ G) Lit: (DMPO-OH: $a_N=a_{\beta-H}=14.9$ G).[32]
Abbreviations: DMPO, 5,5-dimethyl-1-pyrroline-*N*-oxide; EPR, electron paramagnetic resonance.

To determine if N-TiO_2 NP and light treatment caused cytotoxicity, as indicated by decreases in cellular metabolism in hGEPs, WST-1 assays, which measure the mitochondrial activity, were performed (Figure 7). Cells were treated with increasing concentrations of N-TiO_2 NPs and immediately exposed to either blue light or ambient light for 60 minutes. Following light exposure, the NPs were aspirated and cellular metabolism was then quantified at 3 (Figure 7A) and 24 hours (Figure 7B) postexposure. After 3 hours, the hGEPs exposed to N-TiO_2 and blue light exhibited significant increases in cellular metabolism when compared to the hGEPS exposed to blue light only. Treatment with N-TiO_2 NPs and ambient light resulted in a slight, yet nonsignificant increase in proliferation as well. Cellular metabolism was significantly elevated in cells exposed to 50 and 100 μg/mL N-TiO_2 NPs for 24 hours, irrespective of light treatment. It appears that N-TiO_2 NPs stimulated cellular metabolism at low and intermediate concentrations, but were not cytotoxic at any concentration tested.

To investigate the potential antibacterial effect of N-TiO_2 NPs and light treatments, the colony counts of *E. coli* after a 60-minute exposure to ambient or blue light in the presence or absence of N-TiO_2 NPs were quantified (Figure 8). Treatment with blue light alone resulted in a significant decrease in *E. coli* colonies. Also, a significant dose-dependent decrease

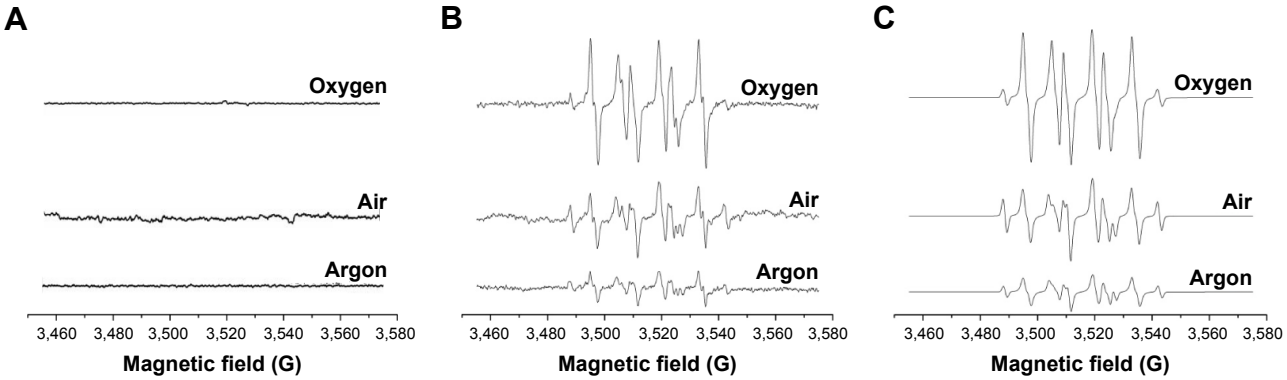

Figure 5 EPR spectra with 1.25 N-TiO_2 in DMPO/DMSO solutions with bubbling of oxygen, air, and argon in (**A**) dark condition (**B**) under visible irradiation, and (**C**) simulated spectra. DMPO-OOH: g=2.0055, a_N=13.9 G, $a_{\beta\text{-}H}$=10.1 G, $a_{\gamma\text{-}H}$=1.4 G; DMPO-alkyl: g=2.0053, a_N=15.8 G, $a_{\beta\text{-}H}$=22.4 G, $a_{\gamma\text{-}H}$=0.6 G.
Notes: Literature values: (DMPO-OOH in DMSO: a_N=12.7 G, $a_{\beta\text{-}H}$=10.3 G, $a_{\gamma\text{-}H}$=1.3 G; DMPO-CH_3 in water/DMSO: a_N=16.1 G, $a_{\beta\text{-}H}$=23.0 G).[32] Simulations correspond to % compositions of % alkyl–% OOH adducts of 7%–93% in oxygen, 17%–83% in air, and 12%–88% in argon.
Abbreviations: DMPO, 5,5-dimethyl-1-pyrroline-*N*-oxide; DMSO, dimethyl sulfoxide; EPR, electron paramagnetic resonance.

in bacterial survival was noted when *E. coli* were exposed to blue light and N-TiO_2 NPs, when compared to exposure under ambient light conditions.

To confirm the antibacterial effect of N-TiO_2 NPs, an additional set of N-TiO_2 NPs and light exposures were performed, and *E. coli* were then subjected to live/dead staining. These confocal fluorescence microscopy studies demonstrated changes in bacterial viability in response to NP exposure. The images shown in Figure 9 reveal a general increase in dead bacteria (red) compared to live bacteria (green) with increasing particle concentration. Damaged bacteria appear to swell and undergo changes in morphology in response to light and particle exposure.

Discussion

Effect of nitrogen doping on TiO_2 structure

Consistent with literature reports,[18–21] nitrogen doping of TiO_2 resulted in absorption extending well into the visible range of wavelengths. The extent of absorption in the visible range of wavelengths was concentration dependent. Adding more nitrogen precursor (ethylmethylamine) resulted in increased visible light absorbance (Figure 1).

There are conflicting literature reports on the mechanism of blue light absorption of N-doped titania. Shifts in the bandgap of TiO_2 have been reported upon nitrogen doping: from 3.45 to 2.75 eV[18] and from 3.2 to 2.4 eV.[34] Other reports

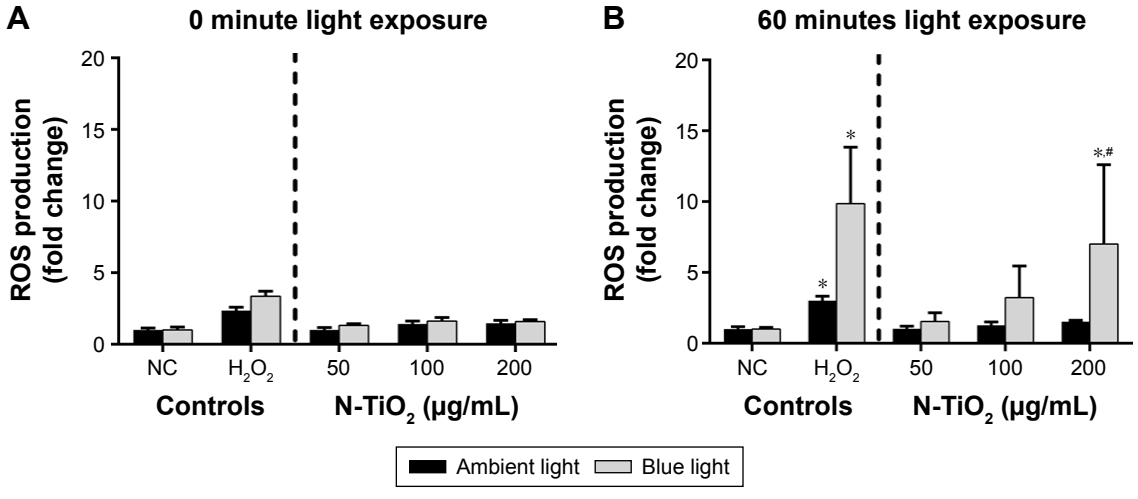

Figure 6 hGEP generation of ROS.
Notes: (**A**) Fold change of ROS production at 0 minute exposure to blue light and ambient light. Exposure to N-TiO_2 NPs normalized to PBS blank. (**B**) Fold change of ROS production after 60 minutes of exposure to ambient light and blue light (485 nm). Exposure to N-TiO_2 NPs normalized to PBS blank for respective light treatments. *Significant difference ($P<0.05$; n=3) between respective NC (light-exposed only) and N-TiO_2-treated cells. #Significant difference ($P<0.05$; n=3) among light treatments at the same NP exposure concentration.
Abbreviations: hGEP, human gingival epithelial cells; NC, negative control; NPs, nanoparticles; PBS, phosphate-buffered saline; ROS, reactive oxygen species.

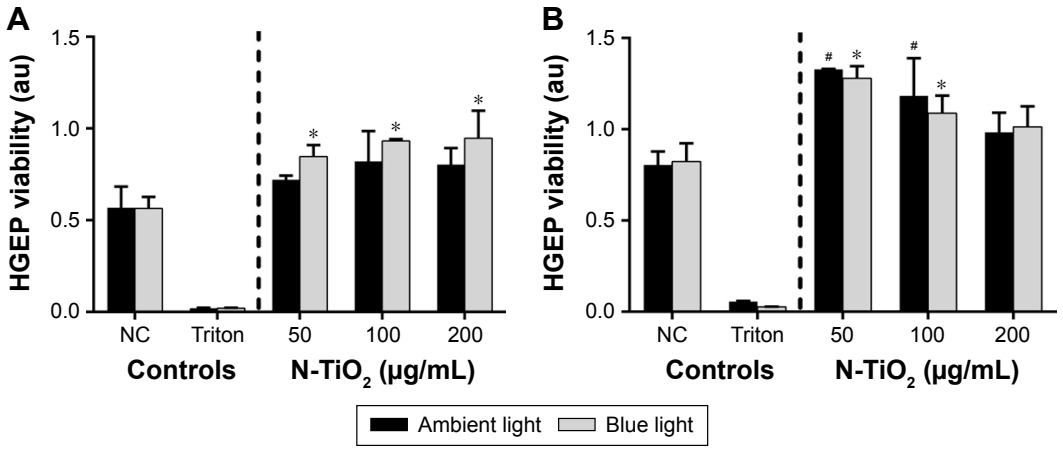

Figure 7 Cellular metabolic responses in hGEPs after N-TiO_2 NP and light exposures.
Notes: (**A**) 3 hours after light and N-TiO_2 NP exposure. (**B**) 24 hours after light and N-TiO_2 NP exposure. *Significant difference between blue light-exposed, non-NP-treated NC and NP treatment. #Significant difference between ambient light-exposed, non-NP-treated NC and NP treatment.
Abbreviations: hGEPs, human gingival epithelial cells; NC, negative control; NP, nanoparticle.

indicate that the bulk material bandgap does not significantly shift, and that the absorption of blue light is instead the result of a variety of states at the valence band edge attributed to titanium-site vacancies and undercoordinated oxygen ions.[19,21] Generally, nitrogen doping by substitution into the crystal structure results in lower energy states closer to the original bandgap, while doping by chemisorption and interstitial incorporation results in deeper trap states. This has generally been found to be dependent on the synthetic method and the concentration of nitrogen precursor, with lower concentrations resulting in substitution and higher concentrations resulting in chemisorption and interstitial doping.[35]

The UV–Vis absorption spectra presented in Figure 1 provide evidence that the increased visible light absorption

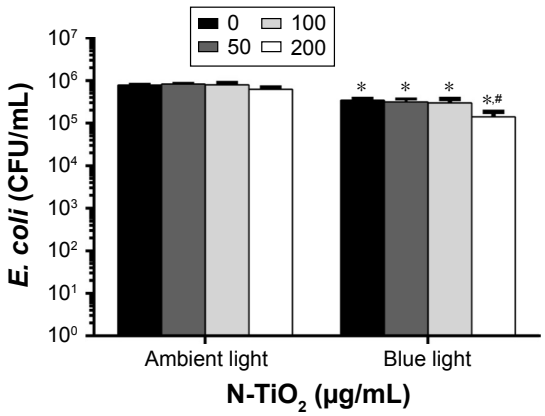

Figure 8 Colony counts of *Escherichia coli* after exposure to 1.25 N-TiO_2 particles and 1 hour of either ambient room light or blue light.
Notes: Bacteria were suspended in PBS during light treatment at a concentration of approximately 10^5, incubated at 37°C for 5 hours, diluted 1:10,000, and plated on lysogeny agar. *Significant difference between blue light-exposed, non-NP-treated NC and NP treatment. #Significant difference between ambient light-exposed, non-NP-treated NC and NP treatment.
Abbreviations: CFU, colony forming units; PBS, phosphate-buffered saline; NC, negative control; NP, nanoparticle.

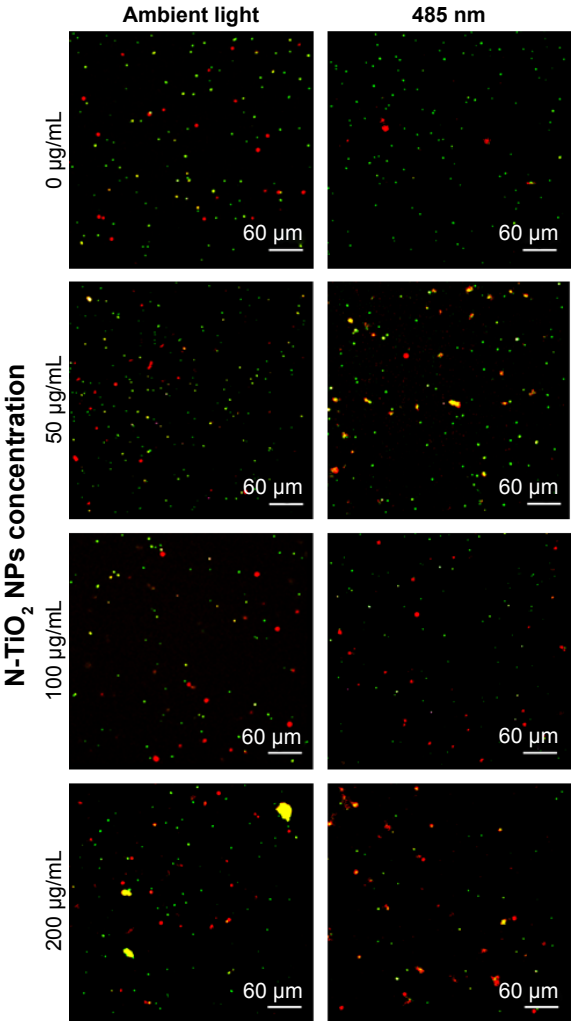

Figure 9 Confocal fluorescence microscopy images of live/dead stained *Escherichia coli* following exposure to N-TiO_2 NPs under either ambient light or 1 hour of exposure to blue light (485 nm).
Notes: Images were taken using a 20× objective. Live bacteria are stained green, while the dead bacteria are stained red.
Abbreviation: NPs, nanoparticles.

in this synthesis can be attributed to valence band trap states. Most of the samples showed no shift in the main bandgap of the material when calculated by Tauc plots (3.11 eV), but did show a tail extending into lower energies characteristic of trap state formation. The Tauc plot calculation for 1.5 N-TiO_2 (2.99 eV) appears to be skewed lower by the increasing amplitude of the trap state peak relative to the main bandgap.

The TEM images presented in Figure 3 show nanosized primary particles of approximately 20–30 nm agglomerated into larger 200–300 nm aggregate particles. It should be noted that the aggregation state of the particles can impact their toxicity, as they have a larger effective hydrodynamic radius than the initial primary particles.[36] As some aggregation was observed, it will be imperative to control dispersal when considering the biological applications for N-TiO_2 NPs as the aggregation state may alter the biocompatibility of the final material.

From zeta potential pH titration data (Figure 10), we find that undoped TiO_2 particles had an IEP of pH 5.2. This matches well with literature: anatase TiO_2 particles were found to have an IEP between pH 5 and 6, depending on their size.[37] The IEP of 1.25 N-TiO_2 shifted to a pH of 4. Literature reports show that the crystal structure of titania does not affect the IEP,[37] meaning this shift was not due to the transformation to rutile phase. Nitrogen doping has been shown to decrease the zeta potentials and IEP of TiO_2.[34,38] We, therefore, conclude that the change in IEP for N-TiO_2 in the present study was due to the addition of nitrogen functionality to the surface.

Next we investigated the ability of the synthesized N-TiO_2 NPs to generate free radicals, which could potentially be exploited to make them an effective antibacterial agent. The appearance of EPR signals upon light irradiation in the presence of N-TiO_2 NPs is attributed to the formation of $^{\bullet}OH$.[39] The formation of $O_2^{\bullet-}$ was not observed due to the short half-life of DMPO-O_2H which decomposes to DMPO-OH, or the fast dismutation of $O_2^{\bullet-}$ to form H_2O_2 and the subsequent metal-catalyzed homolytic cleavage of H_2O_2 to $^{\bullet}OH$ to form DMPO-OH.[40] Superoxide adduct of DMPO has been shown to be more persistent in DMSO[41]; hence, spin trapping was performed in aqueous DMSO solution. Comparison of the relative levels of radicals formed in air- versus O_2-bubbled suspensions shows higher levels of $O_2^{\bullet-}$ adduct in O_2-bubbled system (93%) than with air bubbling (83%) while higher $^{\bullet}CH_3$ level was observed in air-bubbling (17%) than in O_2 (7%) and that these signals are significantly decreased with Ar-bubbling.

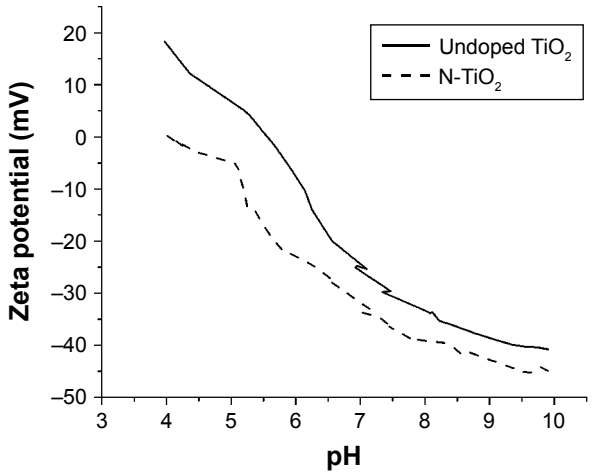

Figure 10 Zeta potential titration versus pH for undoped TiO_2 NPs and N-TiO_2 NPs.
Abbreviation: NPs, nanoparticles.

Biocompatibility and antibacterial activity of N-TiO_2 NPs

Advancements in the materials engineering field have led to the release of hundreds of consumer products that contain nanomaterials.[42] Applications capitalizing on the unique ability of TiO_2 NPs to form ROS under UV light irradiation are of particular interest. However, UV light is damaging and repeated exposure has been linked to skin damage and tumors caused directly by UV irradiation and indirectly through oxidative stress mechanisms and uncontrolled ROS formation.[43] Furthermore, while the cytotoxicity and oxidative stress responses after exposure to undoped TiO_2 have been extensively studied,[44–47] the biological effects of N-TiO_2 NPs exposure are less understood. Thus, in addition to thoroughly characterizing the properties of N-TiO_2 NPs in a cell-free environment, we also sought to elucidate the antibacterial effects of N-TiO_2 NPs and determine their initial biocompatibility in a normal human cell culture model.

The ROS assays (Figure 6) demonstrate that N-TiO_2 NPs exposed to blue light induce dose-dependent ROS generation in hGEPs compared to PBS-negative controls. There was a significant change in ROS production between ambient and blue light treatments after exposure to the highest dosage (200 μg/mL) of N-TiO_2 NPs. Although there are relatively few investigations which report on ROS production of N-TiO_2 NPs in mammalian cell models, our ROS results match those described in Li et al's report,[48] which compared the cytotoxicity of undoped and N-doped TiO_2 NPs in HeLa cells. In the aforementioned studies, irradiation with blue light (400–440 nm) for up to 5 minutes resulted in substantial increases in total ROS as well as superoxide and hydroxyl radical formation at similar concentrations to those used in our study. As demonstrated through EPR (Figures 4 and 5) studies, the primary ROS generated under visible light exposure were hydroxyl and superoxide radicals. However, there

are conflicting literature reports on the production of ROS by nitrogen-doped TiO_2. Some reports agree with our finding that superoxide radicals are produced,[30,48] while others indicate that carbon-centered radicals are produced.[19] Nonetheless, the presence of free radicals indicates that cells may be exposed to conditions that promote oxidative stress, which could result in adverse cellular responses including cell death. To begin to understand what, if any, effects the N-TiO_2 NPs may have on normal human cells, metabolic activity measurements in hGEPs were performed immediately (3 hours) or after a 24-hour recovery period.

Interferences have been reported for several types of assays used to estimate cytotoxicity, proliferation, and mitochondrial activity. Specifically, there is a known binding activity between TiO_2 and lactate dehydrogenase, which is the commonly used cytotoxicity assay.[49,50] TiO_2 also caused noncellular reduction in the 3-(4,5-dimethylthiazol-2-yl)-2,5-diphenyltetrazolium bromide assay.[51] In the current study, WST-1 was selected as an indicator of metabolic activity assay because cell-free testing using NPs alone and the WST-1 reagent did not result in any artifacts or interferences, which suggests that WST-1 is a suitable indicator of cellular metabolism and, therefore, can be used as an indirect measure of cellular viability. The metabolic activity of hGEPs increased significantly within 3 hours of light and N-TiO_2 NP exposure, which suggests that the ROS may induce enhanced metabolism in response to these stimuli, due to the cells actively working to neutralize any oxidative stress associated with this treatment. Interestingly, the same trend was noted for cells exposed to N-TiO_2 NPs 24 hours after irradiation with ambient or blue light, except at the highest concentration tested. These data suggest that N-TiO_2 NPs may generate ROS at levels that stimulate mitochondrial activity and increased cellular metabolism, but the cells are equipped with enough antioxidant mechanisms to protect them and preserve their viability. These data are in agreement with Behzadnia et al,[52] who demonstrated no adverse effects when fabrics treated with N-TiO_2 NPs were exposed to normal human dermal fibroblasts. Yet, the findings in the present study are also in contrast with the viability and cellular responses reported in other studies. As described earlier, Li et al reported significant increases in ROS.[48] However, in their study, they also demonstrate decline in HeLa cell mitochondrial membrane potential and significant increases in intracellular Ca^{2+} levels, both of which are indicative of severe cytotoxicity. Furthermore, in a previous study, the same group demonstrated that N-TiO_2 NPs are capable of inducing cytotoxicity and micronuclei formation in three cancer cell lines.[53] There are several notable differences between our study and the studies of Li. One such difference is the intensity and duration of light used among the studies. The present study used 12.85 mW/cm^2 for 60 minutes, and Li irradiated with 12 mW/cm^2 for 4 hours or 40 mW/cm^2 for up to 5 minutes in his studies. Also, the particles were prepared using ammonia gas as a nitrogen source. Finally, the cell culture models employed by these authors were cancer cell lines, which often have various susceptibilities to different stimuli, compared with the normal cells used in this study. As such, the work presented here indicates that while the N-TiO_2 NPs induce ROS, the normal cells may be equipped with adequate protective mechanisms to ensure their survival. Further studies are warranted to investigate potential cellular responses after repeated or chronic exposure to both light and N-TiO_2 NPs.

Multiple studies have demonstrated the antibacterial effects of undoped TiO_2 NPs alone and under UV irradiation.[14,54,55] Several groups have demonstrated effective bacterial and fungal reduction using N-TiO_2 NPs and films.[56–58] In the present work, a repeatable, dose-dependent (0–200 μg/mL) toxicity toward *E. coli* resulted upon blue light treatment (Figure 8). An approximately 1-log reduction in bacterial population was observed with the highest concentration of particles. These findings were in agreement with the morphological changes and the decrease in number of viable bacteria observed by confocal microscopy. The antibacterial activity reported here is not as substantial as reported by Cao et al, where 90% reduction was observed in *Lactobacillus acidophilus* and *Candida albicans*.[58] Their study was performed using a much longer 24-hour exposure to visible light and a thin film surface of nitrogen-doped titania. Furthermore, it is possible that ROS scavenging occurred, minimizing the potency of oxidative stress.

Conclusion

The N-TiO_2 NPs synthesized by this method produced ROS (hydroxyl and superoxide) capable of significantly reducing bacterial counts while maintaining the viability of human epithelial cells, in the presence of water, oxygen, and visible light. Subsequent experiments will determine if the N-TiO_2 NPs are toxic to biofilm-forming bacteria (*S. mutans*) when incorporated into a dental resin composite material. While blue light exposure alone induced ROS production in hGEPs, this is not considered prohibitive toward the eventual use of these particles in dental applications. A current barrier to the

translation of these particles into a real-life application is the length of light exposure and the depth of light penetration required to achieve an impactful biological effect. One-hour light exposures were required to exhibit antibacterial activity at the concentrations used in solution against planktonic bacteria. In the resin formulation, particle concentrations can be >50% by weight of the material. It is expected that light exposure times required to achieve antibacterial activity will be reduced. Therefore, future work is aimed at reducing the irradiation times and enhancing the antibacterial effects while maintaining a balance of oxidative stress that is toxic to bacteria and minimally affecting mammalian cellular responses.

Acknowledgments

The authors wish to thank Ms Shannon Olsen for her lab managerial assistance and assay refinement efforts and Mr Duane Cox for his expert engineering skills used to construct the light box. The authors also wish to acknowledge Mr Tony Yuan and Mr Matt Morgan for their assistance with processing the confocal images. In addition, the authors thank Dr Amer Tiba for his critical feedback and thoughtful discussion.

Disclosure

The views expressed in this article are those of the authors and do not necessarily reflect the official policy or position of the Department of the Navy, Department of Defense, or the US Government. Title 17 U.S.C. §105 provides that "Copyright protection under this title is not available for any work of the United States Government". Title 17 U.S.C. §101 defines a US Government work as a work prepared by a military service member or employee of the US Government, as part of that person's official duties. This work was funded by the Naval Medical Research Center's Advanced Medical Development Program using work unit number G1405. Amber Nagy is an employee of the US Government and Andrew Zane, Ann Marie Digeorge Foushee, and Kristin Flores are contracted by the US Government. This work was prepared as part of our official duties. Ranfang Zuo was supported by Fundamental Research Funds for the Central Universities (Grant No 2652013037). The Hungarian National Research, Development and Innovation Office (NKFIH) Grant Nr. K119442 is acknowledged for support of Antal Rockenbauer.

The authors report no other conflicts of interest in this work.

References

1. McCracken MS, Gordan VV, Litaker MS, et al. A 24-month evaluation of amalgam and resin-based composite restorations: findings from The National Dental Practice-Based Research Network. *J Am Dent Assoc*. 2013;144(6):583–593.
2. Drummond JL. Degradation, fatigue and failure of resin dental composite materials. *J Dent Res*. 2008;87(8):710–719.
3. Brunthaler A, König F, Lucas T, Sperr W, Schedle A. Longevity of direct resin composite restorations in posterior teeth. *Clin Oral Investig*. 2003;7(2):63–70.
4. Li Y, Carrera C, Chen R, et al. Degradation in the dentin-composite interface subjected to multi-species biofilm challenges. *Acta Biomater*. 2014;10(1).375–383.
5. Mutluay MM, Zhang K, Ryou H, et al. On the fatigue behavior of resin-dentin bonds after degradation by biofilm. *J Mech Behav Biomed Mater*. 2013;18:219–231.
6. Shen W, Zhang C, Li Q, Zhang W, Cao L, Ye J. Preparation of titanium dioxide nano particle modified photocatalytic self-cleaning concrete. *J Clean Prod*. 2015;87:762–765.
7. Sakhuja M, Son J, Yang H, Bhatia CS, Danner AJ. Outdoor performance and durability testing of antireflecting and self-cleaning glass for photovoltaic applications. *Sol Energ*. 2014;110:231–238.
8. Gant RM, Hou Y, Grunlan MA, Coté GL. Development of a self-cleaning sensor membrane for implantable biosensors. *J Biomed Mater Res*. 2009;90A(3):695–701.
9. Ohko Y, Utsumi Y, Niwa C, et al. Self-sterilizing and self-cleaning of silicone catheters coated with TiO2 photocatalyst thin films: a preclinical work. *J Biomed Mater Res*. 2001;58(1):97–101.
10. Kulkarni M, Mazare A, Gongadze E, et al. Titanium nanostructures for biomedical applications. *Nanotechnology*. 2015;26(6):062002.
11. Linsebigler AL, Lu G, Yates JT. Photocatalysis on TiO_2 surfaces: principles, mechanisms, and selected results. *Chem Rev*. 1995;95(3):735–758.
12. Gupta K, Singh RP, Pandey A, Pandey A. Photocatalytic antibacterial performance of TiO_2 and Ag-doped TiO_2 against *S. aureus*. *P. aeruginosa* and *E. coli*. *Beilstein J Nanotechnol*. 2013;4:345–351.
13. Lee WS, Park YS, Cho YK. Significantly enhanced antibacterial activity of TiO2 nanofibers with hierarchical nanostructures and controlled crystallinity. *Analyst*. 2014;140(2):616–622.
14. Joost U, Juganson K, Visnapuu M, et al. Photocatalytic antibacterial activity of nano-TiO2 (anatase)-based thin films: effects on *Escherichia coli* cells and fatty acids. *J Photochem Photobiol B*. 2015;142:178–185.
15. Ermis RB, Yildirim D, Yildiz G, Gormez O. Radiopacity evaluation of contemporary resin composites by digitization of images. *Eur J Dent*. 2014;8(3):342–347.
16. Wu J, Weir MD, Melo MA, Xu HH. Development of novel self-healing and antibacterial dental composite containing calcium phosphate nanoparticles. *J Dent*. 2015;43(3):317–326.
17. Huyang G, Sun J. Clinically applicable self-healing dental resin composites. *MRS Advances*. 2016;1(08):547–552.
18. Jagadale TC, Takale SP, Sonawane RS, et al. N-doped TiO2 nanoparticle based visible light photocatalyst by modified peroxide sol−gel method. *J Phys Chem C*. 2008;112(37):14595–14602.
19. Mrowetz M, Balcerski W, Colussi AJ, Hoffmann MR. Oxidative power of nitrogen-doped TiO2 photocatalysts under visible illumination. *J Phys Chem B*. 2004;108(45):17269–17273.
20. Wang G, Xiao X, Li W, et al. Significantly enhanced visible light photoelectrochemical activity in TiO2 nanowire arrays by nitrogen implantation. *Nano Lett*. 2015;15(7):4692–4698.
21. Chen H, Dawson JA. Nature of nitrogen-doped anatase TiO_2 and the origin of its visible-light activity. *J Phys Chem C*. 2015;119(28):15890–15895.
22. Janpetch N, Vanichvattanadecha C, Rujiravanit R. Photocatalytic disinfection of water by bacterial cellulose/N–F co-doped TiO2 under fluorescent light. *Cellulose*. 2015;22(5):3321–3335.

23. Pongwan P, Wetchakun K, Phanichphant S, Wetchakun N. Enhancement of visible-light photocatalytic activity of Cu-doped TiO2 nanoparticles. *Res Chem Intermed*. 2016;42:2815–2830.
24. Ashkarran AA, Hamidinezhad H, Haddadi H, Mahmoudi M. Double-doped TiO2 nanoparticles as an efficient visible-light-active photocatalyst and antibacterial agent under solar simulated light. *Appl Surf Sci*. 2014;301:338–345.
25. Sato K, Taguchi H, Maeda T, et al. The primary cytotoxicity in ultraviolet-a-irradiated riboflavin solution is derived from hydrogen peroxide. *J Investig Dermatol*. 1995;105(4):608–612.
26. Zaleska A. Doped-TiO_2: a review. *Recent Pat Biomed Eng*. 2008;2(3):157–164.
27. Asahi R, Morikawa T, Irie H, Ohwaki T. Nitrogen-doped titanium dioxide as visible-light-sensitive photocatalyst: designs, developments, and prospects. *Chem Rev*. 2014;114(19):9824–9852.
28. Hernández-Sierra JF, Galicia-Cruz O, Angélica S-A, Ruiz F, Pierdant-Pérez M, Pozos-Guillén AJ. In vitro cytotoxicity of silver nanoparticles on human periodontal fibroblasts. *J Clin Pediatr Dent*. 2011;36(1):37–41.
29. Taleghani F, Yaraii R, Sadeghi R, Haghgoo R, Rezvani MB. Cytotoxicity of silver nanoparticles on human gingival epithelial cells: an in-vitro study. *Shahid Beheshti Univ Dent J*. 2014;32(1):30–36.
30. Fu H, Zhang L, Zhang S, Zhu Y, Zhao J. Electron spin resonance spin-trapping detection of radical intermediates in N-doped TiO2-assisted photodegradation of 4-chlorophenol. *J Phys Chem B*. 2006;110(7):3061–3065.
31. Rockenbauer A, Korecz L. Automatic computer simulations of ESR spectra. *Appl Magn Reson*. 1996;10(1–3):29–43.
32. Buettner GR. Spin trapping: ESR parameters of spin adducts 1474 1528V. *Free Rad Biol Med*. 1987;3(4):259–303.
33. Kohno M, Mizuta Y, Kusai M, Masumizu T, Makino K. Measurements of superoxide anion radical and superoxide anion scavenging activity by electron spin resonance spectroscopy coupled with DMPO spin trapping. *Bull Chem Soc Jpn*. 1994;67(4):1085–1090.
34. Ha S-J, Kim DH, Moon JH. N-doped mesoporous inverse opal structures for visible-light photocatalysts. *RSC Adv*. 2015;5(95):77716–77722.
35. Viswanathan B, Krishanmurthy KR. Nitrogen incorporation in TiO2: does it make a visible light photo-active material? *Int J Photoenergy*. 2012;2012:e269654.
36. Jiang J, Oberdörster G, Biswas P. Characterization of size, surface charge, and agglomeration state of nanoparticle dispersions for toxicological studies. *J Nanopart Res*. 2008;11(1):77–89.
37. Suttiponparnit K, Jiang J, Sahu M, Suvachittanont S, Charinpanitkul T, Biswas P. Role of surface area, primary particle size, and crystal phase on titanium dioxide nanoparticle dispersion properties. *Nanoscale Res Lett*. 2010;6(1):27.
38. Miyauchi M, Ikezawa A, Tobimatsu H, Irie H, Hashimoto K. Zeta potential and photocatalytic activity of nitrogen doped TiO_2 thin films. *Phys Chem Chem Phys*. 2004;6(4):865–870.
39. Villamena FA, Hadad CM, Zweier JL. Kinetic study and theoretical analysis of hydroxyl radical trapping and spin adduct decay of alkoxycarbonyl and dialkoxyphosphoryl nitrones in aqueous media. *J Phys Chem A*. 2003;107(22):4407–4414.
40. Villamena FA, Merle JK, Hadad CM, Zweier JL. Superoxide radical anion adduct of 5,5-dimethyl-1-pyrroline N-oxide (DMPO). 1. The thermodynamics of formation and its acidity. *J Phys Chem A*. 2005;109(27):6083–6088.
41. Harbour JR, Hair ML. Detection of superoxide ions in nonaqueous media. Generation by photolysis of pigment dispersions. *J Phys Chem*. 1978;82(12):1397–1399.
42. Contado C. Nanomaterials in consumer products: a challenging analytical problem. *Front Chem*. 2015;3:48.
43. Ichihashi M, Ueda M, Budiyanto A, et al. UV-induced skin damage. *Toxicology*. 2003;189(1–2):21–39.
44. Cai R, Kubota Y, Shuin T, Sakai H, Hashimoto K, Fujishima A. Induction of cytotoxicity by photoexcited TiO_2 particles. *Cancer Res*. 1992;52(8):2346–2348.
45. Wamer WG, Yin JJ, Wei RR. Oxidative damage to nucleic acids photosensitized by titanium dioxide. *Free Radic Biol Med*. 1997;23(6):851–858.
46. Shukla RK, Sharma V, Pandey AK, Singh S, Sultana S, Dhawan A. ROS-mediated genotoxicity induced by titanium dioxide nanoparticles in human epidermal cells. *Toxicol In Vitro*. 2011;25(1):231–241.
47. Shukla RK, Kumar A, Gurbani D, Pandey AK, Singh S, Dhawan A. TiO(2) nanoparticles induce oxidative DNA damage and apoptosis in human liver cells. *Nanotoxicology*. 2013;7(1):48–60.
48. Li Z, Pan X, Wang T, Wang PN, Chen JY, Mi L. Comparison of the killing effects between nitrogen-doped and pure TiO_2 on HeLa cells with visible light irradiation. *Nanoscale Res Lett*. 2013;8(1):96.
49. Zaqout MSK, Sumizawa T, Igisu H, Wilson D, Myojo T, Ueno S. Binding of titanium dioxide nanoparticles to lactate dehydrogenase. *Environ Health Prev Med*. 2012;17(4):341–345.
50. Han X, Gelein R, Corson N, et al. Validation of an LDH assay for assessing nanoparticle toxicity. *Toxicology*. 2011;287(1–3):99–104.
51. Lupu AR, Popescu T. The noncellular reduction of MTT tetrazolium salt by TiO_2 nanoparticles and its implications for cytotoxicity assays. *Toxicol In Vitro*. 2013;27(5):1445–1450.
52. Behzadnia A, Montazer M, Rashidi A, Mahmoudi Rad M. Rapid sonosynthesis of N-doped nano TiO_2 on wool fabric at low temperature: introducing self-cleaning, hydrophilicity, antibacterial/antifungal properties with low alkali solubility, yellowness and cytotoxicity. *Photochem Photobiol*. 2014;90(6):1224–1233.
53. Li Z, Mi L, Wang PN, Chen JY. Study on the visible-light-induced photokilling effect of nitrogen-doped TiO_2 nanoparticles on cancer cells. *Nanoscale Res Lett*. 2011;6(1):356.
54. Petersen EJ, Reipa V, Watson SS, Stanley DL, Rabb SA, Nelson BC. DNA damaging potential of photoactivated p25 titanium dioxide nanoparticles. *Chem Res Toxicol*. 2014;27(10):1877–1884.
55. Pleskova SN, Golubeva IS, Verevkin YK. Bactericidal activity of titanium dioxide ultraviolet-induced films. *Mater Sci Eng C Mater Biol Appl*. 2016;59:807–817.
56. Wong MS, Chu WC, Sun DS, et al. Visible-light-induced bactericidal activity of a nitrogen-doped titanium photocatalyst against human pathogens. *Appl Environ Microbiol*. 2006;72(9):6111–6116.
57. Li Q, Xie R, Li YW, Mintz EA, Shang JK. Enhanced visible-light-induced photocatalytic disinfection of *E. coli* by carbon-sensitized nitrogen-doped titanium oxide. *Environ Sci Technol*. 2007;41(14):5050–5056.
58. Cao S, Liu B, Fan L, Yue Z, Liu B, Cao B. Highly antibacterial activity of N-doped TiO_2 thin films coated on stainless steel brackets under visible light irradiation. *Appl Surf Sci*. 2014;309:119–127.